

# Optical parameters of oxide films typically used in optical coating production

Alexander V. Tikhonravov,<sup>1,\*</sup> Michael K. Trubetskov,<sup>1</sup> Tatiana V. Amotchkina,<sup>1</sup>  
Gary DeBell,<sup>2</sup> Vladimir Pervak,<sup>3</sup> Anna Krasilnikova Sytchkova,<sup>4</sup>  
Maria Luisa Grilli,<sup>4</sup> and Detlev Ristau<sup>5</sup>

<sup>1</sup>Research Computing Center, Moscow State University, Leninskie Gory, 119992, Moscow, Russia

<sup>2</sup>MLD Technologies, 2672 Bayshore Parkway, Suite 701, Mountain View, California 94043, USA

<sup>3</sup>Ludwig-Maximilians-Universitaet München, Am Coulombwall 1, D-85748 Garching, Germany

<sup>4</sup>National Agency for New Technologies, Energy, and the Environment (ENEA),  
Optical Coatings Group, Via Anguillarese 301, 00123 Rome, Italy

<sup>5</sup>Laser Zentrum Hannover e.V., Department of Thin Film Technology,  
Hollerithallee 8, 30419 Hannover, Germany

\*Corresponding author: tikh@srcc.msu.ru

Received 30 July 2010; accepted 8 September 2010;  
posted 22 September 2010 (Doc. ID 132608); published 25 October 2010

Wavelength dependencies of refractive indices of thin film materials differ for various deposition conditions, and it is practically impossible to attribute a single refractive index wavelength dependence to any typical thin film material. Besides objective reasons, differences in the optical parameters of thin films may also be connected with nonadequate choices of models and algorithms used for the processing of measurement data. The main goal of this paper is to present reliable wavelength dependencies of refractive indices of the most widely used slightly absorbing oxide thin film materials. These dependencies can be used by other researchers for comparison and verification of their own characterization results. © 2010 Optical Society of America

*OCIS codes:* 310.3840, 310.6860.

## 1. Introduction

Despite an old history of optical characterization of thin films, this topic is still at the center of interest of the optical coatings community. Evidence of this fact is that at the last three Optical Interference Coatings (OIC) Topical Meetings in 2004, 2007, and 2010, special measurement problems were added to the traditional design and manufacturing problems [1–3]. Unlike bulk material refractive indices, there are still no commonly used databases providing spectral dependencies of thin film material refractive indices. An absence of such databases and permanent

interest in optical characterization of thin films are connected with the fact that it is practically impossible to attribute a single refractive index wavelength dependence to any typical thin film material. Optical parameters of thin films are very much dependent on a type of deposition process and on specific parameters of this process [4,5].

Besides the above-mentioned objective reason, there are also other reasons for obtaining different optical parameters of the same thin film material by different researchers. There are differences in the measurement data used and the accuracy of these data and differences in models and algorithms applied for extracting the optical parameters of thin films from experimental information. Depending on the choices of measurement data, a thin film model

and algorithm for data processing of various characterization results can be obtained. This was clearly demonstrated in Ref. [6], where results from several laboratories for analogous thin film samples were presented and compared.

In what follows, we shall refer to a combination of the measurement data used, thin film model, and algorithm for data processing for a characterization approach. A useful classification of a great variety of existing characterization approaches was proposed in Ref. [7]. According to this classification, all approaches are subdivided into single- and multiwavelength approaches. Typical examples of single-wavelength approaches can be found in Refs. [8–11]. They are based on successive determinations of the refractive index ( $n$ ) and extinction coefficient ( $k$ ) values at every wavelength where measurement data are available. These data are typically reflectance ( $R$ ) and transmittance ( $T$ ) data. Specific approaches differ mainly by algorithms used for extracting  $n$  and  $k$  values from  $R$  and  $T$  values.

Multiwavelength characterization approaches are currently the most widely used. They are based on the fitting of measured reflectance and transmittance curves by respective theoretical spectral dependencies calculated in the frame of some chosen thin film model [7]. A great portion of multiwavelength characterization approaches is based on the minimization of a function estimating the discrepancy between measured and model spectral curves [6,7]. In what follows, we call such a function a discrepancy function. Parameters of a thin film model providing the minimum value of a discrepancy function are usually considered as searched-for optical parameters of investigated thin film [7].

Results obtained by the minimization of the discrepancy function are dependent on the choice of a thin film model. For example, refractive index wavelength dependencies obtained in the frames of homogeneous and inhomogeneous film models may differ considerably [12–14]. Thus a proper choice of a thin film model is one of the key issues for thin film characterization.

The choice of a thin film model is dependent on the type of available measurement data. For example, it may be difficult to accurately determine the thin film extinction coefficient if only transmittance data are available for thin film characterization [15]. In principle, applying more sophisticated thin film models requires using wider combinations of photometric data [16].

Because different types of measurement data and different thin film models used for data processing may give different characterization results, verification of these results is required [17,18]. Several approaches to such verification were discussed in Ref. [18]. Knowing the influence of systematic and random errors in measurement data on characterization results is also important for estimating the validity and accuracy of these results [17,19].

The main goal of this paper is to present reliable wavelength dependencies of refractive indices of the most widely used oxide thin film materials in the visible spectral range. In connection with the above-discussed issues, the presentation of any refractive index wavelength dependence is accompanied by the descriptions of the deposition technique, measurement data, and thin film model applied for data processing. In fact, we make an attempt to provide some sort of database of thin film refractive indices that can be used by other researchers for comparison and verification of their own characterization results.

To explain why specific thin film models are used for data processing, in Section 2 we provide a short summary of the main results related to a theoretically substantiated choice of a thin film model. In Section 3 we provide examples of a methodology of data processing aimed at obtaining the most reliable characterization results. The wavelength dependencies of refractive indices of six thin film oxide materials are presented in Section 4. Final conclusions are given in Section 5.

## 2. Theoretical Results Related to the Choice of Thin Film Model

In this paper we limit our considerations to high-quality dielectric films. The term high-quality means here that films can be only slightly absorbing, that they are rather dense, and, as a consequence, their bulk inhomogeneity is not too big and surface micro-roughness is not too high. Oxide thin films used for visible applications obviously fall into this category. Theoretical results considered in this section are related to the influence of low absorption, low bulk inhomogeneity, and low surface roughness on spectral properties of such dielectric thin films.

One of the most important theoretical results is traced back to the early history of thin film optics. In 1941 the German scientist Schröder derived an approximation for the reflection coefficient of a slightly inhomogeneous dielectric film [20]. The physical ideas used by Schröder in his derivations are illustrated by Fig. 1. Schröder assumed that the refractive index of inhomogeneous film is smooth and

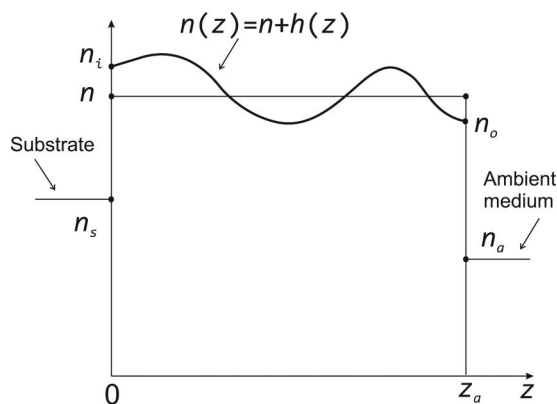


Fig. 1. Schematic of a slightly inhomogeneous dielectric thin film.

varies slightly from the mean refractive index value  $n$ . Under this assumption, all interference effects connected with the refractive index inhomogeneity inside the film can be ignored and only interference effects connected with the abrupt variations of the refractive index at the film boundaries should be taken into account.

In the frame of the Schröder approximation, a specific type of refractive index variation from its mean value is not essential. Carniglia showed [21] that this approximation can be derived, assuming that the film refractive index varies linearly between the  $n_i$  and  $n_o$  values. An incline of the linear refractive index profile can be characterized by the value

$$\delta = \frac{n_o - n_i}{n}, \quad (1)$$

which is usually called the degree of film inhomogeneity.

One can see from Eq. (1) that in the case of a positive degree of inhomogeneity, the film refractive index increases from the substrate boundary to the outer boundary while in the case of a negative degree of inhomogeneity, it decreases in this direction.

The degree of film inhomogeneity is a convenient parameter for representing the bulk inhomogeneity of dielectric thin films. It is often presented in a percentage scale. To obtain a percentage value of  $\delta$ , one should multiply Eq. (1) by 100%.

Using the mean refractive index value  $n$  and the degree of inhomogeneity  $\delta$ , the main equation of the Schröder approximation can be represented in the following form:

$$r = \frac{\left[ (n_a - n_s) - \frac{\delta}{2}(n_a + n_s) \right] \cos \varphi + i \left( \frac{n_a n_s}{n} - n \right) \sin \varphi}{\left[ (n_a + n_s) - \frac{\delta}{2}(n_a - n_s) \right] \cos \varphi + i \left( \frac{n_a n_s}{n} + n \right) \sin \varphi}. \quad (2)$$

Twenty years after the original Schröder work, Koppelman and Krebs used this approximation to obtain their famous conclusions related to the shifts of spectral characteristics of inhomogeneous thin films [22]. It was shown in Ref. [22] that in the case when the film refractive index  $n$  is higher than the substrate refractive index  $n_s$ , a film inhomogeneity results in shifts of the transmittance maxima from the transmittance of the uncoated substrate. In the case when  $n$  is less than  $n_s$ , transmittance minima are shifted from the uncoated substrate transmittance. These conclusions are illustrated in Figs. 2 and 3.

Figures 2 and 3 show shifts of transmittance extrema in the case of a positive degree of inhomogeneity. In the case of negative  $\delta$  values, these extrema are shifted in the opposite direction. The equation for variations of transmittance extrema is as follows:

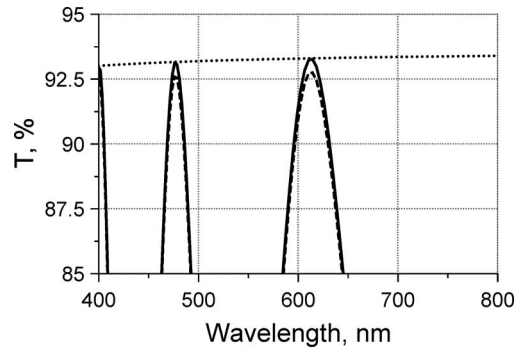


Fig. 2. Shifts of transmittance maxima from the transmittance of the uncoated substrate in the case of  $n > n_s$  and positive film inhomogeneity (a model niobium pentoxide film with physical thickness of 400 nm on quartz substrate is used as an example): solid curve, transmittance of a homogeneous film; dashed curve, transmittance in the case of  $\delta = 3\%$ ; and dotted curve, transmittance of the uncoated substrate.

$$\delta T = -\frac{4n_a n_s (n_a - n_s)}{(n_a + n_s)^3} \delta. \quad (3)$$

In the case  $n > n_s$ , this equation gives variations of the transmittance maxima  $\delta T_{\max}$ , and, in the case of  $n < n_s$ , it gives variations of the transmittance minima  $\delta T_{\min}$ .

Analogous conclusions are valid with respect to the reflectance extrema. In the case of  $n > n_s$ , the reflectance minima are shifted from the reflectance of the uncoated substrate, and, in the case of  $n < n_s$ , reflectance maxima are shifted from this curve. Respective variations  $\delta R_{\min}$  and  $\delta R_{\max}$  are given by the same expression as in Eq. (3) but with the plus sign.

An attractive feature of the Schröder approximation is that it allows describing bulk inhomogeneity with only one parameter—degree of inhomogeneity  $\delta$ . As discussed in the next section, this enables one to specify a model of an inhomogeneous thin film in a simple and physically sensible way.

In Ref. [15], the influence of small absorption losses on spectral coefficients of a thin film was considered and equations for variations of reflectance and transmittance caused by these losses were

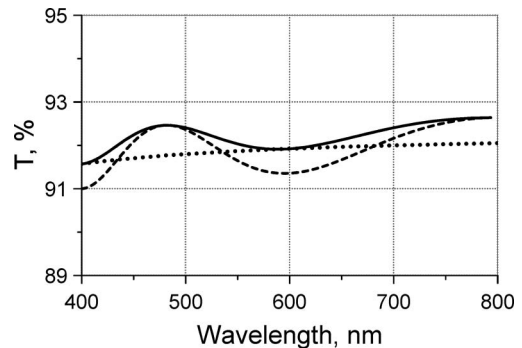


Fig. 3. Shifts of transmittance minima from the transmittance of the uncoated substrate in the case of  $n < n_s$  and positive film inhomogeneity (a model silicon dioxide film with physical thickness of 400 nm on BK7 substrate is used as an example): solid curve, transmittance of a homogeneous film; dashed curve, transmittance in the case of  $\delta = 3\%$ ; and dotted curve, transmittance of the uncoated substrate.

derived. It follows from these equations that only a spatial integral value of the film extinction coefficient has an effect on  $R$  and  $T$  variations. Therefore, it might be practically impossible to determine a spatial variation of a small absorption inside a film.

Another important conclusion of Ref. [15] is that for typical dielectric thin films, a small absorption affects the spectral reflectance much less than it affects the spectral transmittance. In other words, spectral reflectance is rather insensitive to a small extinction coefficient. Therefore, applying thin film models, taking into account the film extinction coefficient, is not reasonable when only reflectance measurements are available.

As the last topic of this section, we discuss the influence of surface roughness on spectral coefficients of a dielectric thin film. A practically oriented description of surface roughness that takes into account the difference of physical effects produced by different spatial harmonics of surface roughness was proposed in Ref. [23]. In that paper, two parameters: small-scale rms roughness  $\sigma_s$  and large-scale rms roughness  $\sigma_l$  were introduced. The terms “small-scale” and “large-scale” are related to spatial roughness harmonics that are small and large compared with the wavelength of the incident light.

Small- and large-scale roughness harmonics produce basically different effects on the reflected and transmitted light. Small-scale roughness does not cause light losses by scattering. It causes only a redistribution of the energy between the reflected and transmitted light beams. Large-scale roughness harmonics causes light scattering in both media surrounding the rough surface, and the sum of specular reflectance and transmittance is not equal to 100% anymore.

Small-scale surface roughness can be caused by the columnar structure of a thin film deposited on a substrate [23,24], while large-scale surface roughness should be first attributed to the inaccuracies of substrate polishing. Atomic force microscopy measurements enable estimating the parameters  $\sigma_s$  and  $\sigma_l$  [23]. For high-quality substrates and thin films, both parameters are less than 1 nm [23–25].

Equations for the variations of reflection and transmission coefficients caused by small- and large-scale roughness can be found in Ref. [23]. For  $\sigma_s$  and  $\sigma_l$  values equal to 1 nm,  $R$  and  $T$  variations and light losses for scattering in the visible spectral region are in the range of several hundred percent. Such variations and losses are definitely below the typical accuracy of measurement data, and it is not necessary to take them into account. Thus, for high-quality thin films, it is not reasonable to include roughness parameters in the thin film model used for characterization in the visible spectral region.

### 3. Methodology of Measurement Data Processing and Verification of Characterization Results

In this section we consider two examples that illustrate the methodology of choosing thin film models

for data processing based on a preliminary analysis of available measurement data. Theoretical results discussed in the previous section are used for this analysis.

The first example is provided by the characterization problem specified for the OIC 2004 meeting [1]. The requirement was to investigate the optical parameters of an unknown single layer deposited on a fused silica substrate using transmittance and reflectance spectra measured at a near normal light incidence. For the goals of this section, thin film material anonymity is not required and it is possible to announce that it was an  $\text{HfO}_2$  layer deposited with Advanced Plasma Source (APS) technology [26].

Measurements of reflectance and transmittance were performed in the spectral range from 200 to 1600 nm with a Cary 500 spectrophotometer at an  $8^\circ$  angle of incidence on the sample. The measured data are shown in Fig. 4.

A very preliminary analysis of data in Fig. 4 tells us that the film material has high absorption near the left wavelength boundary of the measurement region because the decrease of transmittance in this region is obviously connected with the film and not with the fused silica substrate, which is still transparent around 200 nm. In the following analysis we exclude some measurements data in the region near 200 nm, where the film is highly absorbing.

Quite useful information about the investigated thin film and also about an accuracy of the measurement data is provided by examining a spectral behavior of the function  $A(\lambda) = 100\% - T(\lambda) - R(\lambda)$ . This function accounts for total losses in the film and substrate. Figure 5 presents the total losses in the spectral region from 225 to 1600 nm. One can see that in the UV region, a spectral behavior of  $A(\lambda)$  is close to that typical for conventional absorption losses in a dielectric film and, thus, conventional extinction coefficient models can be applied in this region.

A ripple of  $A(\lambda)$  to the left from 1400 nm is obviously connected with the presence of water in the fused silica substrate. Except for this ripple, a spectral behavior of  $A(\lambda)$  above 800 nm is quite unusual. Both the film and substrate have only very small

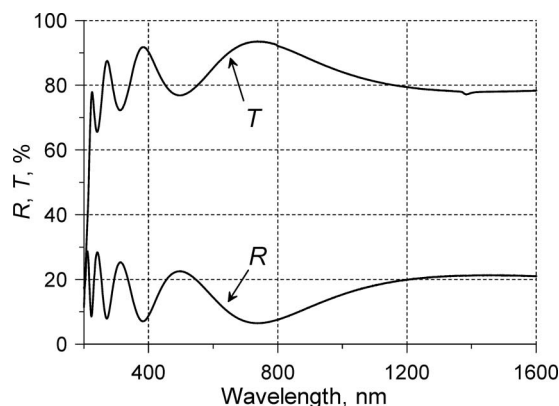


Fig. 4. Reflectance and transmittance of the  $\text{HfO}_2$  sample on a fused silica substrate at  $8^\circ$  in the 200 to 1600 nm spectral region.

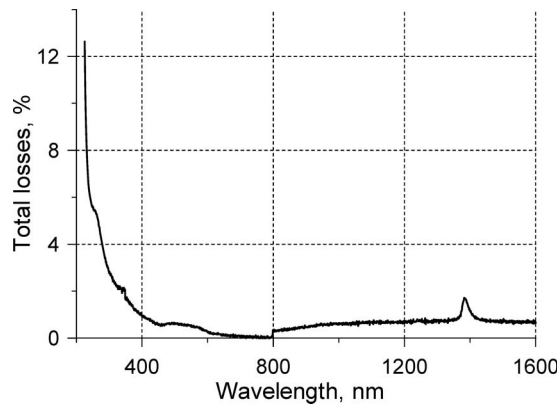


Fig. 5. Total losses in the film and substrate in the spectral region from 225 to 1600 nm.

absorption losses in this region, and losses by scattering are also not possible because of the high quality of the substrate used.

The only explanation for a strange behavior of  $A(\lambda)$  above 800 nm is a presence of systematic errors either in the  $T$  or  $R$  measurement data. At 800 nm, the spectrophotometric light detector is changed for a less reliable one and this explanation is quite reasonable. We shall discuss what data are affected by the detector later in this section. At the moment we would like only to underline that systematic errors in measurement data are especially dangerous for thin film characterization [17,19]. For this reason we now truncate our measurement data to the spectral region from 225 to 800 nm. We shall discuss determining the refractive index wavelength dependence in a wide spectral region a little bit later.

The next step of analyzing measurement data for choosing a thin film model is a comparison of the measured reflectance and transmittance data with the reflectance and transmittance of the uncoated substrate (see Fig. 6). The maximum of the measured transmittance near 740 nm coincides with the transmittance of the uncoated substrate. The deviations of two other transmittance maxima down from this curve should be attributed to the absorption in thin

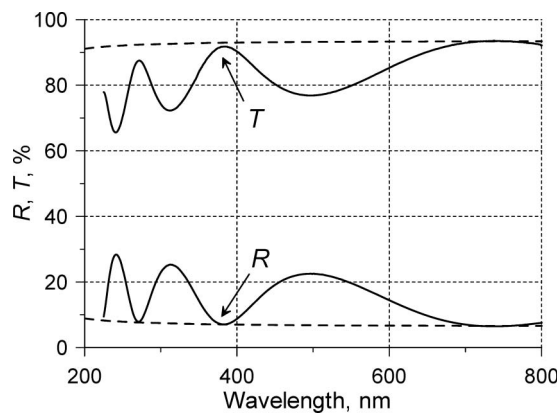


Fig. 6. Comparison of measured reflectance and transmittance data in the 225 to 800 nm spectral region with reflectance and transmittance of the uncoated fused silica substrate.

film and not to thin film inhomogeneity. An additional assurance that the film is fairly homogeneous is provided by the examination of the measured reflectance data. According to Section 2, reflectance data are much less influenced by a small absorption than are transmittance data and, indeed, all minima of the measured reflectance are close to the reflectance of the uncoated substrate. Their deviations from this curve are in the range of 0.1%–0.2%, which does not exceed an estimated accuracy of reflectance measurement data. Thus the application of homogeneous film models for processing of measurement data is well justified now.

For processing of  $T$  and  $R$  measurement data in the 225 to 800 nm spectral region, we use a homogeneous thin film model that incorporates the following models for  $n(\lambda)$  and  $k(\lambda)$ :

$$n(\lambda) = n_{\infty} + \frac{A}{\lambda^2} + \frac{B}{\lambda^4}, \quad k(\lambda) = B_0 \exp(-B_1/\lambda - B_2\lambda). \quad (4)$$

According to our experience, this model works quite well in the visible spectral region for slightly absorbing thin films with extinction coefficient values below 0.01 in this region. Equation (4) contains six model parameters. The seventh unknown model parameter is the film physical thickness,  $h$ . The actual parameters of the film are found by the minimization of the discrepancy function estimating the closeness of measured  $R$  and  $T$  data to respective model data. OptiChar characterization software is used for this purpose [27]. The fitting of measurement data by the model transmittance and reflectance curves at the end of the discrepancy function minimization is shown in Fig. 7. The obtained wavelength dependencies of the refractive index and extinction coefficients are depicted in Fig. 8. The film physical thickness is found to be equal to 190.9 nm.

It might be interesting to find the refractive index wavelength dependence in the spectral region above 800 nm. Recall that either  $T$  or  $R$  data contain systematic errors in this region. A detailed examination

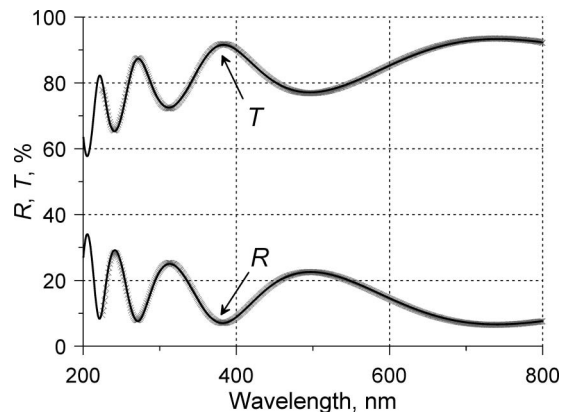


Fig. 7. Fitting of measured reflectance and transmittance data in the 225 to 800 nm spectral region (gray crosses) by model reflectance and transmittance (solid curves) at the end of the discrepancy function minimization: absorbing model of  $\text{HfO}_2$  film.

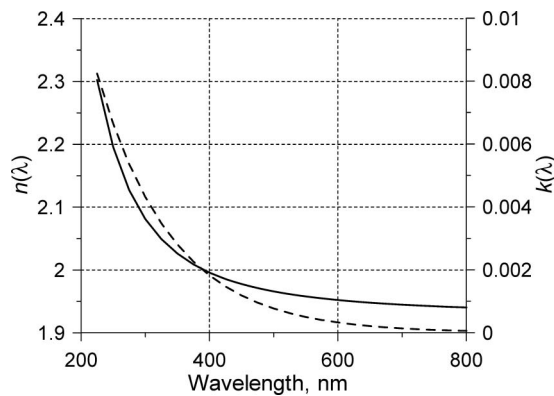


Fig. 8. Wavelength dependencies of the refractive index (solid curve) and extinction coefficient (dashed curve) of the  $\text{HfO}_2$  film found in the frame of the absorbing thin film model based on  $R$  and  $T$  data.

of measurement data indicates that there is a leap of measured  $T$  data around 800 nm. Thus, systematic errors are associated with the transmittance data and if one wants to use these data for optical characterization above 800 nm, it would be required to improve the accuracy of transmittance data above 800 nm. An alternative would be to use only reflectance data for further processing.

According to Section 2, reflectance data are rather insensitive to small absorption in a thin film. Therefore, we simplify a model for data processing by excluding the extinction coefficient parameter from the model. The remaining parameters are thin film physical thickness and the three parameters of the Cauchy dispersion formula for  $n(\lambda)$  [see Eq. (4)].

It should be noted here that unjustified complication of a thin film model and the increase of a number of unknown parameters may easily lead to the instability of model parameter determination. This instability usually reveals itself in obtaining physically not sensible optical parameters of a thin film.

We apply the nonabsorbing four-parametric thin film model for processing reflectance measurement data in the spectral region from 250 to 1600 nm where total losses are less than 5.5% (see Fig. 5). The fitting of measurement data at the end of the discrepancy function minimization is shown in Fig. 9. The obtained wavelength dependence of the film refractive index is depicted in Fig. 10 (solid curve). The film physical thickness is found to be equal to 191.2 nm.

The dashed curve in Fig. 10 shows the previously found refractive index wavelength dependence that was obtained in the frame of the absorbing thin film model based on  $R$  and  $T$  data. One can observe a good correspondence between the results obtained in the frames of two different thin film models. The difference between the two refractive index curves does not exceed 0.4% in the spectral region from 275 to 800 nm. The difference in the obtained physical thickness values is even less (only 0.16%). Such self-verification of the characterization results raises assurance of their correctness.

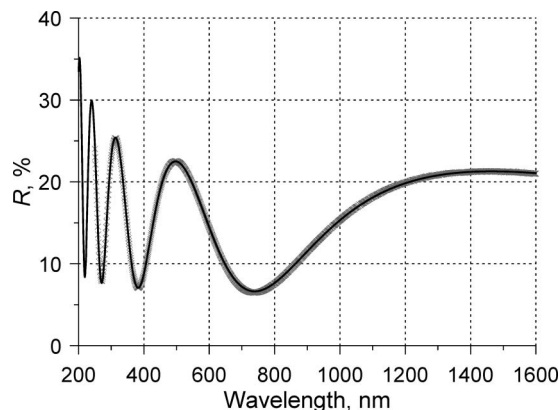


Fig. 9. Fitting of measured reflectance data (gray crosses) by model reflectance (solid curve) at the end of discrepancy function minimization: nonabsorbing model of  $\text{HfO}_2$  film.

Consider one more example of choosing a thin film model based on the analysis of measurement data. In this case we have only transmittance data measured in the spectral region from 400 to 1600 nm for the niobium pentoxide film on a fused silica substrate. The film was deposited on a superpolished fused silica substrate using an ion beam sputtering process. Transmittance measurements were made with a Cary 500 spectrophotometer for the spectral region where neither film nor substrate have noticeable absorption except for the substrate water absorption band near 1380 nm. The measurements were made with a reference to the uncoated substrate placed in the reference arm of the spectrophotometer. For this reason, measured transmittance data have no ripple around 1380 nm.

Measured data are shown by crosses in Fig. 11. The solid curve in this figure represents transmittance of the uncoated fused silica substrate. Note that the shift of the measured transmittance maximum from the transmittance of the uncoated substrate observed in this figure is about 0.5%. An estimated accuracy of transmittance data below

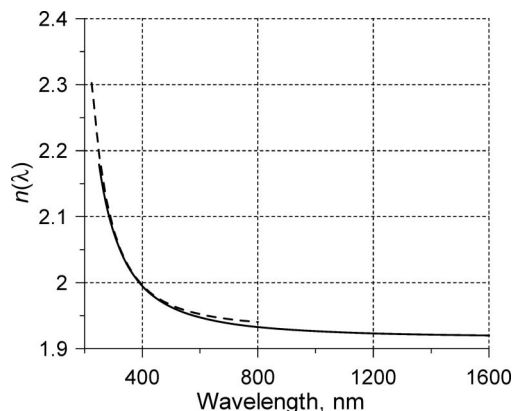


Fig. 10. Wavelength dependencies of the refractive index of  $\text{HfO}_2$  film found in the frame of nonabsorbing thin film model based on  $R$  data (solid curve). Dashed curve shows the wavelength dependence found in the frame of the absorbing model based on  $R$  and  $T$  data.

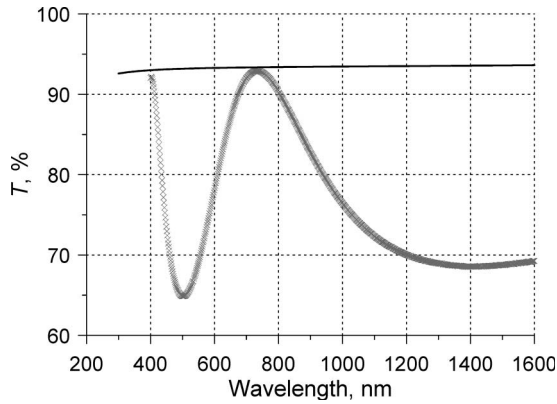


Fig. 11. Transmittance of the niobium pentoxide film on the fused silica substrate (gray crosses) and transmittance of the uncoated substrate (solid curve).

800 nm is about 0.1%. So the observed shift of the transmittance maximum cannot be connected with measurement errors. It cannot be caused by absorption or scattering losses because we use a high-quality substrate and niobium pentoxide is non-absorbing in the considered spectral region. Thus it is necessary to conclude that the shift of the transmittance maximum is caused by bulk inhomogeneity of the discussed film sample.

The introduction of models for inhomogeneous thin films was discussed in Ref. [15]. In general the refractive index of a film that is inhomogeneous along its thickness should be described by the function of two variables  $n(z, \lambda)$ . Such a function is, however, inconvenient for further parametrization. For this reason it was proposed to present the refractive index of a slightly inhomogeneous thin film in the form [15]

$$n(z, \lambda) = q(z)n(\lambda), \quad (5)$$

where  $n(\lambda)$  is the mean refractive index of inhomogeneous film and  $q(z)$  is the function describing film inhomogeneity. This function was called the inhomogeneity factor.

Equation (5) separates the description of a bulk inhomogeneity from the description of a dispersive behavior of the film refractive index, and its further parametrization is quite straightforward. As discussed in Section 2 in the case of the Schröder inhomogeneity model, it is enough to represent inhomogeneity by a single parameter called the degree of film inhomogeneity. This is equivalent to the introduction of a linear inhomogeneity factor. Using the degree of film inhomogeneity  $\delta$ , the inhomogeneity factor  $q(z)$  is introduced by the equation

$$q(z) = 1 + \delta(z/h - 1/2), \quad (6)$$

where  $h$  is the physical thickness of the inhomogeneous film.

For the description of the dispersive behavior of the mean refractive index  $n(\lambda)$ , any one of the commonly used parametric models can be applied. To

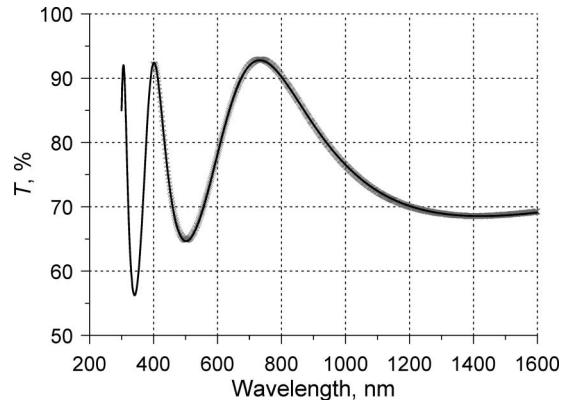


Fig. 12. Fitting of measured transmittance data (gray crosses) by model transmittance (solid curve) obtained in the frame of the inhomogeneous model of  $\text{Nb}_2\text{O}_5$  film.

process measurement data shown in Fig. 11, we choose a standard three-parametric Cauchy model [see Eq. (4)]. Thus, on a whole we have five unknown model parameters. These are three parameters of the Cauchy model, the degree of inhomogeneity  $\delta$ , and the film physical thickness  $h$ .

As before, the actual parameters of the investigated niobium pentoxide film are found by the minimization of the discrepancy function, and OptiChar characterization software is used for this purpose. The fitting of the measured transmittance by the model transmittance at the end of the discrepancy function minimization is shown in Fig. 12. The obtained wavelength dependence of the film refractive index is presented in Fig. 13 by the solid curve. The film physical thickness and degree of film inhomogeneity are found to be equal to 161.9 nm and 3.2%, respectively.

Verification of the obtained characterization results is always important. For the first sample considered in this section, a self-verification of results was demonstrated. A verification based on previously obtained results for other samples of the same thin film material is also possible. As discussed in Refs. [18,19], there are no physical reasons

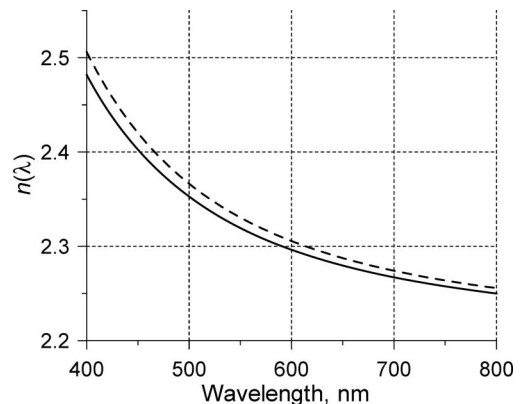


Fig. 13. Wavelength dependence of the refractive index of the  $\text{Nb}_2\text{O}_5$  film found in the frame of the inhomogeneous thin film model (solid curve). The dashed curve shows the wavelength dependence of the refractive index of  $\text{Nb}_2\text{O}_5$  from Ref. [28].

Table 1. Summary of Information Related to the Thin Film Samples Whose Refractive Index Wavelength Dependencies Are Presented in Figs. 14–19

Film Material	Sample Number	Deposition Process	Measurement Data Spectral Region (nm)	Model	Film Thickness, nm	Degree of Inhomogeneity (%)	$n(\lambda)$	$n(500)$	Discrepancy Function (%)
HfO <sub>2</sub>	1	OIC 2004 APS technology	<i>R</i> , <i>T</i> 225–800	absorbing homogeneous	190.9	0	Fig. 14	1.966	0.29
HfO <sub>2</sub>	2	RF sputtering	<i>R</i> , <i>T</i> 250–1200	absorbing inhomogeneous	200.7	2.5	Fig. 14	1.984	0.27
HfO <sub>2</sub>	3	ion beam sputtering	<i>R</i> , <i>T</i> 300–850	absorbing homogeneous	213.1	0	Fig. 14	2.129	0.12
Nb <sub>2</sub> O <sub>5</sub>	1	ion beam sputtering	<i>T</i> 400–1600	nonabsorbing inhomogeneous	161.9	3.2	Fig. 15	2.353	0.14
Nb <sub>2</sub> O <sub>5</sub>	2	ac magnetron sputtering	Ellipsometric data at 65° 400–850	nonabsorbing inhomogeneous surface overlay	423.2	1.6	Fig. 15	2.366	2.25
Nb <sub>2</sub> O <sub>5</sub>	3	magnetron sputtering	<i>T</i> 400–820	nonabsorbing homogeneous	305.4	0	Fig. 15	2.367	0.15
Ta <sub>2</sub> O <sub>5</sub>	1	magnetron sputtering	<i>T</i> 400–820	nonabsorbing homogeneous	337.5	0	Fig. 16	2.164	0.07
Ta <sub>2</sub> O <sub>5</sub>	2	ion beam sputtering	<i>T</i> 300–2000	nonabsorbing inhomogeneous	191.5	2.7	Fig. 16	2.137	0.35
Ta <sub>2</sub> O <sub>5</sub>	3	RF magnetron sputtering	<i>T</i> 400–1200	nonabsorbing homogeneous	298.7	0	Fig. 16	2.156	0.26
SiO <sub>2</sub>	1	magnetron sputtering	<i>T</i> 400–820	nonabsorbing homogeneous	294.8	0	Fig. 17	1.471	0.02
SiO <sub>2</sub>	2	ion beam sputtering	<i>R</i> 400–1200	nonabsorbing homogeneous	538.3	0	Fig. 17	1.495	0.06
Al <sub>2</sub> O <sub>3</sub>	1	RF sputtering	<i>R</i> , <i>T</i> 250–850	absorbing inhomogeneous	205.5	1.2	Fig. 18	1.654	0.1
Al <sub>2</sub> O <sub>3</sub>	2	ion beam sputtering	<i>R</i> 300–850	nonabsorbing homogeneous	721.8	0	Fig. 18	1.675	0.05
TiO <sub>2</sub>	1	ion beam sputtering	<i>R</i> , <i>T</i> 400–850	absorbing homogeneous	507.3	0	Fig. 19	2.508	0.4
TiO <sub>2</sub>	2	electron beam evaporation	<i>T</i> 400–850	nonabsorbing homogeneous	176.5	0	Fig. 19	2.358	0.08

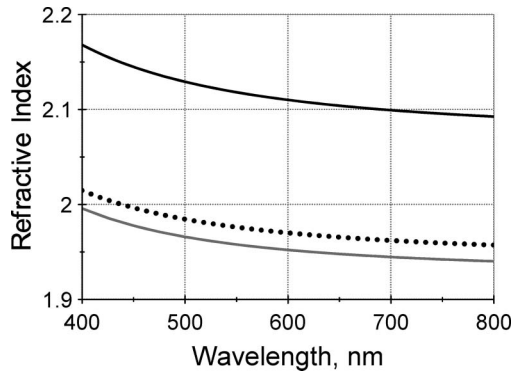


Fig. 14. Refractive indices of  $\text{HfO}_2$  films produced by ion beam sputtering (solid curve), RF sputtering (dotted curve), and APS technology (gray curve).

for basically different types of refractive index wavelength dependencies of several samples of the same amorphous thin film material produced in different deposition environments. Variations of film density result mainly in shifts of refractive index wavelength dependencies up or down. More dense films should, of course, exhibit higher refractive index values.

For the verification of the obtained refractive index wavelength dependence (solid curve in Fig. 13), we use the refractive index wavelength dependence of  $\text{Nb}_2\text{O}_5$  film presented in Ref. [28]. This dependence is shown in Fig. 13 by a dashed curve.

The film sample from Ref. [28] was deposited by ac magnetron sputtering on a fused silica substrate with a thickness of approximately 500 nm. Measurement data were ellipsometric data obtained with a Woollam ellipsometer in the spectral region from 400 to 850 nm at a  $65^\circ$  angle of incidence. For the processing of ellipsometric data, an inhomogeneous film model was applied. This model had one additional parameter compared to the model used in this paper. This parameter was a thickness of a surface overlayer representing small-scale surface roughness [23,28,29]. An introduction of this additional parameter was connected with a high sensitivity of ellipsometric data to small-scale roughness. The film

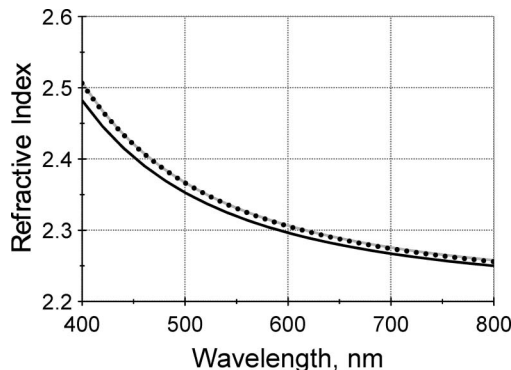


Fig. 15. Refractive indices of  $\text{Nb}_2\text{O}_5$  films produced by ion beam sputtering (solid curve), ac magnetron sputtering (dotted curve), and magnetron sputtering in the Helios coater (gray curve): note that the second and third dependencies are almost undistinguished.

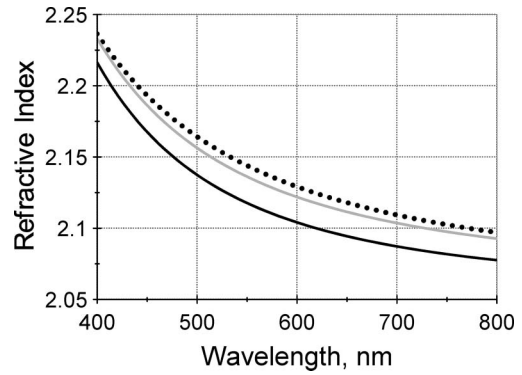


Fig. 16. Refractive indices of  $\text{Ta}_2\text{O}_5$  films produced by ion beam sputtering (solid curve), magnetron sputtering in the Helios coater (dotted curve), and RF magnetron sputtering (gray curve).

physical thickness, the degree of inhomogeneity, and the overlayer thickness were found equal to 423.2 nm, 1.6%, and 1.2 nm, respectively.

It is not surprising that the refractive index wavelength dependence found in Ref. [28] is somewhat different from that found in this paper. Recall that the  $\text{Nb}_2\text{O}_5$  film considered in this paper was deposited using ion beam sputtering, while the  $\text{Nb}_2\text{O}_5$  film from Ref. [28] was deposited using ac magnetron sputtering. According to Fig. 13, the second film is denser than the first film.

In Ref. [28] and in this paper, different measurement data were used for thin film characterization. The models applied for data processing were also different. Nevertheless, the patterns of the found refractive index wavelength dependencies are similar. This gives an assurance in the correctness of the obtained results.

#### 4. Refractive Indices of Typical Oxide Thin Film Materials

In this section we provide a summary of results related to wavelength dependencies of refractive indices of the most widely used oxide thin film materials. This summary incorporates some of our previous results presented in several publications. But most of the presented results are new. Respective

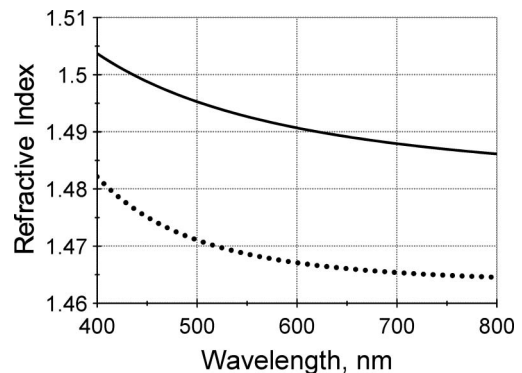


Fig. 17. Refractive indices of  $\text{SiO}_2$  films produced by ion beam sputtering (solid curve) and magnetron sputtering in the Helios coater (dotted curve).

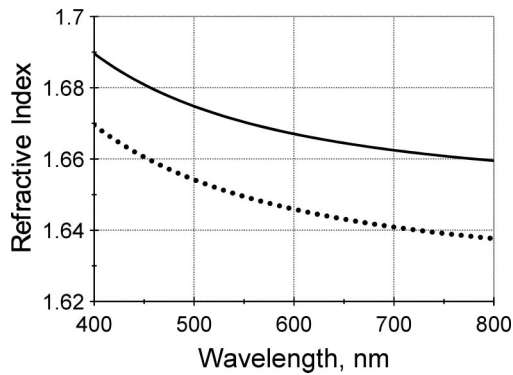


Fig. 18. Refractive indices of  $\text{Al}_2\text{O}_3$  films produced by ion beam sputtering (solid curve) and RF sputtering (dotted curve).

samples were deposited and measured specifically for this paper.

Spectral photometric measurements for the new samples were performed in the spectral region somewhat broader than the visible spectral region. Thin film models for data processing were chosen according to the methodology discussed in the previous section. Table 1 lists all new and previously investigated samples and provides the most essential information related to these samples. In particular, the deposition technique, type, and spectral region of measurement data used and the chosen model are indicated for each sample. In the last column of Table 1, the discrepancy function values at the end of the minimization procedures are presented. These values represent the root mean square deviations of the model data from the measured data, in percent. Wavelength dependencies of the refractive indices are presented in Figs. 14–19 for each thin film material separately. Because different samples of the same oxide thin film material were produced using different deposition techniques, their refractive indices typically differ. At the same time, the results presented in Figs. 14–19 demonstrate good correspondences between the types of wavelength dependencies of the refractive indices of various samples of the same material. Sometimes there is even an amazing coincidence between the refractive indices of samples deposited using different techniques.

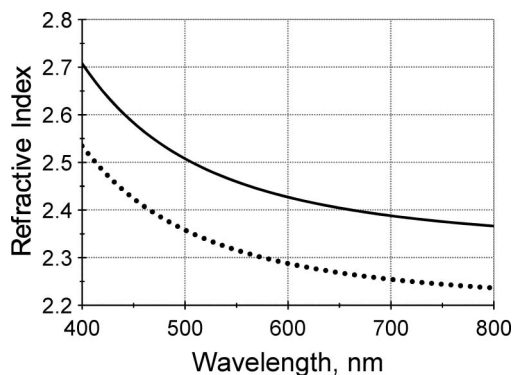


Fig. 19. Refractive indices of  $\text{TiO}_2$  films produced by ion beam sputtering (solid curve) and electron beam evaporation (dotted curve).

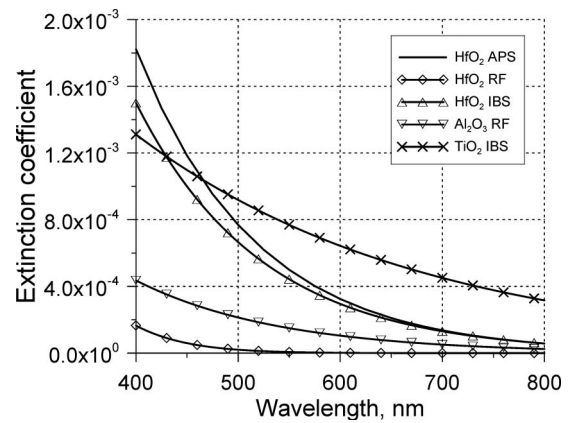


Fig. 20. Extinction coefficients of  $\text{HfO}_2$  films produced by APS technology, RF sputtering, and ion beam sputtering of  $\text{Al}_2\text{O}_3$  film produced by RF sputtering and of  $\text{TiO}_2$  film produced by ion beam sputtering.

Results presented in this section can provide guidelines for choosing thin film models for determining refractive indices of other samples of oxide thin film materials. They can be also used for comparison and verification of refractive index wavelength dependencies found for other samples. For such comparison, additional information about the samples of this section is required. For this reason, Table 1 provides also physical thicknesses of all investigated samples and found values of the degree of inhomogeneity when inhomogeneous thin film models were used for data processing. Wavelength dependencies of extinction coefficients of  $\text{HfO}_2$ ,  $\text{Al}_2\text{O}_3$ , and  $\text{TiO}_2$  films found in the cases of absorbing thin film models are presented in Fig. 20.

## 5. Conclusions

It is practically impossible to attribute a single refractive index wavelength dependence to any thin film material because their refractive indices depend on deposition conditions. For this reason, there are no commonly used databases of refractive indices of thin film materials. It is, however, possible to create a reference database that can be used for comparison and verification of characterization results obtained for thin film materials. This paper presents such a database for six oxide thin film materials that are widely used in optical coating production.

Despite a seeming simplicity of extracting optical parameters of thin films from optical characterization data, the analysis of available measurement data is not a straightforward formal procedure. For the correctness of this analysis, a proper choice of thin film model is crucial. This choice must be correlated with the available experimental information and its accuracy. This paper summarizes the most important theoretical results that are required for a well-grounded choice of a thin film model and presents examples of the methodology of processing measurement data.

This work was supported by the Deutsche Forschungsgemeinschaft (DFG) Cluster of Excellence,

“Munich Centre for Advanced Photonics” (<http://www.munich-photonics.de>) and by the Russian Foundation for Basic Research (RFBR), projects 09-02-13607 and 10-07-00480a (<http://www.rfbr.ru>).

## References

1. A. Duparré and D. Ristau, “2004 Topical Meeting on Optical Interference Coatings: Measurement Problem,” in *Optical Interference Coatings*, OSA Technical Digest Series (Optical Society of America, 2004), paper WD1.
2. A. Duparré and D. Ristau, “Optical Interference Coatings 2007 Measurement Problem,” *Appl. Opt.* **47**, C179–C184 (2008).
3. A. Duparré and D. Ristau, “2010 OSA Topical Meeting on Optical Interference Coatings: Measurement Problem,” in *Optical Interference Coatings*, OSA Technical Digest Series (Optical Society of America, 2010), paper ThC1.
4. M. Friz and F. Waibel, “Coating materials,” in N. Kaiser and H. K. Pulker, eds., *Optical Interference Coatings* (Springer-Verlag, 2003), pp. 105–130.
5. B. T. Sullivan and J. A. Dobrowolski, “Deposition error compensation for optical multilayer coatings. I. theoretical description,” *Appl. Opt.* **31**, 3821–3835 (1992).
6. D. P. Arndt, R. M. A. Azzam, J. M. Bennett, J. P. Borgogno, C. K. Carniglia, W. E. Case, J. A. Dobrowolski, U. J. Gibson, T. Tuttle Hart, F. C. Ho, V. A. Hodgkin, W. P. Klapp, H. A. Macleod, E. Pelletier, M. K. Purvis, D. M. Quinn, D. H. Strome, R. Swenson, P. A. Temple, and T. F. Thonn, “Multiple determination of the optical constants of thin-film coating materials,” *Appl. Opt.* **23**, 3571–3596 (1984).
7. J. A. Dobrowolski, F. C. Ho, and A. Waldorf, “Determination of optical constants of thin film coating materials based on inverse synthesis,” *Appl. Opt.* **22**, 3191–3200 (1983).
8. W. E. Case, “Algebraic method for extracting thin-film optical parameters from spectrophotometer measurements,” *Appl. Opt.* **22**, 1832–1836 (1983).
9. L. Vriens and W. Rippens, “Optical constants of absorbing thin solid films on a substrate,” *Appl. Opt.* **22**, 4105–4110 (1983).
10. R. C. McPhedran, L. C. Botten, D. R. McKenzie, and R. P. Netterfield, “Unambiguous determination of optical constants of absorbing films by reflectance and transmittance measurements,” *Appl. Opt.* **23**, 1197–1205 (1984).
11. T. C. Paulick, “Inversion of normal-incidence ( $R, T$ ) measurements to obtain  $n + ik$  for thin films,” *Appl. Opt.* **25**, 562–564 (1986).
12. J. P. Borgogno, P. Bousquet, F. Flory, B. Lazarides, E. Pelletier, and P. Roche, “Inhomogeneity in films: limitation of the accuracy of optical monitoring of thin films,” *Appl. Opt.* **20**, 90–94 (1981).
13. J. P. Borgogno, B. Lazarides, and E. Pelletier, “Automatic determination of optical constants of inhomogeneous thin films,” *Appl. Opt.* **21**, 4020–4029 (1982).
14. J. P. Borgogno, F. Flory, P. Roche, B. Schmitt, G. Albrand, E. Pelletier, and H. A. Macleod, “Refractive index and inhomogeneity of thin films,” *Appl. Opt.* **23**, 3567–3570 (1984).
15. A. V. Tikhonravov, M. K. Trubetskov, B. T. Sullivan, and J. A. Dobrowolski, “Influence of small inhomogeneities on the spectral characteristics of single thin films,” *Appl. Opt.* **36**, 7188–7199 (1997).
16. T. Babeva, S. Kitova, and I. Konstantinov, “Photometric methods for determining the optical constants and the thicknesses of thin absorbing films: selection of a combination of photometric quantities on the basis of error analysis,” *Appl. Opt.* **40**, 2675–2681 (2001).
17. A. Tikhonravov, M. Trubetskov, and G. DeBell, “On the accuracy of optical thin film parameter determination based on spectrophotometric data,” *Proc. SPIE* **5188**, 190–199 (2003).
18. A. Tikhonravov, M. Trubetskov, T. Amotchkina, A. Tikhonravov, D. Ristau, and S. Gunster, “Reliable determination of wavelength dependence of thin film refractive index,” *Proc. SPIE* **5188**, 331–342 (2003).
19. A. V. Tikhonravov, M. K. Trubetskov, M. A. Kokarev, T. V. Amotchkina, A. Duparré, E. Quesnel, D. Ristau, and S. Günster, “Effect of systematic errors in spectral photometric data on the accuracy of determination of optical parameters of dielectric thin films,” *Appl. Opt.* **41**, 2555–2560 (2002).
20. H. Schröder, “Bemerkung zur Theorie des Lichtdurchgangs durch inhomogene durchsichtige Schichten,” *Ann. Phys.* **39**, 55–58 (1941).
21. C. K. Carniglia, “Ellipsometric calculations for nonabsorbing thin films with linear refractive-index gradients,” *J. Opt. Soc. Am. A* **7**, 848–856 (1990).
22. G. Koppelman and K. Krebs, “Die Optischen Eigenschaften Dielektrischer Schichten mit Kleinen Homogenitätsstörungen,” *Z. Phys. D* **164**, 539–556 (1961).
23. A. V. Tikhonravov, M. K. Trubetskov, A. A. Tikhonravov, and A. Duparre, “Effects of interface roughness on the spectral properties of thin films and multilayers,” *Appl. Opt.* **42**, 5140–5148 (2003).
24. J. Ferre-Borrull, A. Duparré, and E. Quesnel, “Procedure to characterize microroughness of optical thin films: application to ion-beam-sputtered vacuum-ultraviolet coatings,” *Appl. Opt.* **40**, 2190–2199 (2001).
25. A. Duparré, J. Ferre-Borrull, S. Gliech, G. Notni, J. Steinert, and J. M. Bennett, “Surface characterization techniques for determining the root-mean-square roughness and power spectral densities of optical components,” *Appl. Opt.* **41**, 154–171 (2002).
26. F. Lemarchand, C. Deumié, M. Zerrad, L. Abel-Tiberini, B. Bertussi, G. Georges, B. Lazarides, M. Cathelinaud, M. Lequime, and C. Amra, “Optical characterization of an unknown single layer: Institut Fresnel contribution to the Optical Interference Coatings 2004 Topical Meeting Measurement Problem,” *Appl. Opt.* **45**, 1312–1318 (2006).
27. A. V. Tikhonravov and M. K. Trubetskov, OptiChar software, <http://www.optilayer.com>.
28. A. V. Tikhonravov, M. K. Trubetskov, G. Clark, B. T. Sullivan, and J. A. Dobrowolski, “Ellipsometric study of optical properties and small inhomogeneities of  $\text{Nb}_2\text{O}_5$  films,” *Proc. SPIE* **3738**, 183–187 (1999).
29. A. V. Tikhonravov, M. K. Trubetskov, and A. V. Krasilnikova, “Spectroscopic ellipsometry of slightly inhomogeneous non-absorbing thin films with arbitrary refractive index profiles: theoretical study,” *Appl. Opt.* **37**, 5902–5911 (1998).